Theoretical analysis of the vapor-liquid-solid mechanism of nanowire growth during molecular beam epitaxy

V. G. Dubrovskii,[1,2,*] N. V. Sibirev,[3] G. E. Cirlin,[1,2,3] J. C. Harmand,[4] and V. M. Ustinov[1,2]
[1]*St.-Petersburg Physical Technical Centre of the Russian Academy of Sciences for Research and Education, Khlopina 8/3, 195220 St.-Petersburg, Russia*
[2]*Ioffe Physical Technical Institute of the Russian Academy of Sciences, Politekhnicheskaya 26, 194021 St.-Petersburg, Russia*
[3]*Institute for Analytical Instrumentation of the Russian Academy of Sciences, Rizhsky 26, 190103 St.-Petersburg, Russia*
[4]*CNRS-LPN, Route de Nozay, 91460 Marcoussis, France*
(Received 11 October 2005; published 14 February 2006)

A theoretical model of nanowire formation by the vapor-liquid-solid mechanism during molecular beam epitaxy and related growth techniques is presented. The model unifies the conventional adsorption-induced model, the diffusion-induced model, and the model of nucleation-mediated growth on the liquid-solid interface. The concentration of deposit atoms in the liquid alloy, the nanowire diameter, and all other characteristics of the growth process are treated dynamically as functions of the growth time. The model provides theoretical length-diameter dependences of nanowires and the dependence of the nanowire length on the technologically controlled growth conditions, such as the surface temperature and the deposition thickness. In particular, it is shown that the length-diameter curves of nanowires might convert from decreasing to increasing at a certain critical diameter and that the nanowires taper when their length becomes comparable with the adatom diffusion length on the sidewalls. The theoretical dependence of the nanowire morphology on its lateral size and length and on the surface temperature are compared to the available experimental data obtained recently for Si and GaAs nanowires.

DOI: 10.1103/PhysRevE.73.021603 PACS number(s): 81.10.Aj, 68.70.+w

I. INTRODUCTION

Renewed interest in the fabrication of semiconductor nanowires, also known as nanowhiskers (NWs), is stimulated by recent advances in their use as building elements for various electronic, optical, and biological applications [1–4]. Techniques of growth of Si [5–7] and III-V [8,9] NWs with a length up to more than 10 μm and a diameter of only few tens of nanometers have been developed and high quality freestanding NW arrays have been obtained. This progress followed several decades of the development of whisker fabrication technology [10–13]. The generally accepted mechanism of whisker formation is usually referred to as vapor-liquid-solid (VLS) growth. The VLS mechanism was introduced in 1964 by Wagner and Ellis [10] for the interpretation of their experiments with chemical vapor deposition (CVD) of Si from $SiCl_4$ on a Si(111) surface activated by Au drops. In 1973, Givargizov and Chernov [14] proposed an empirical model of VLS growth during CVD. The VLS mechanism, originally established for large whiskers with a micrometer scale diameter, has subsequently been used for explaining the formation of different semiconductor NWs [15–17].

In the traditional adsorption-induced VLS model [10,11,14] the following growth behavior is assumed. When the surface is activated by a metal growth catalyst and heated above the eutectic melting point, small drops of the metal form a liquid alloy with the semiconductor material and act as a seed for NW growth. The direct impingement of deposit material from vapors around the drop makes this alloy supersaturated. Semiconductor atoms travel to the liquid-solid interface due to the volume diffusion within the liquid drop. The interface acts as a sink for deposit particles dissolved in the drop, causing their incorporation into the available adsorption sites of the lattice. This leads to vertical growth of the whisker with the drop of liquid alloy sitting on the top. In the diffusion-induced VLS model [18,19] it is assumed that, in addition to the direct impingement, atoms may also arrive at the drop from the substrate surface due to diffusion along the whisker sidewalls. These atoms first dissolve in the drop, then diffuse to the interface, and finally also incorporate into the lattice. Both models described here were recently discussed by Bhunia and co-workers in the case of InP NWs [20], where the additional pathway for deposit particles to travel toward the interface along the drop surface was taken into account.

At the moment semiconductor NWs are most often grown by CVD [1–9]. However, the molecular beam epitaxy (MBE) technique has recently demonstrated its potential for studying the growth mechanisms of Si [21] and GaAs [22,23] NWs in more detail. The MBE technique involves a simple impinging species and the NW formation mechanisms are more easily described by a theoretical model, since no precursor decomposition mechanisms are required. In addition, the MBE technique may provide a number of advantages for NW fabrication technology due to strongly nonequilibrium conditions during MBE growth [24]. In particular, MBE-grown NWs may have a larger length and aspect ratio at a lower material consumption [23]. On the other hand, the un-

*Electronic address: dubrovskii@mail.ioffe.ru

derstanding of NW formation mechanisms during MBE is still at an early stage.

The aim of this paper is the theoretical investigation of NW growth during MBE on surfaces activated by drops of a growth catalyst. In contrast to the recent analysis by Persson and co-workers [25], in this work it is assumed that all drops always remain liquid during the growth, or, in other words, the NW formation proceeds by the VLS mechanism. We will present a generalized dynamical model of NW formation during MBE that takes into account (i) adsorption and desorption processes on the drop surface; (ii) diffusion of atoms from the substrate surface to the drop along the NW sidewalls; (iii) crystal growth on the liquid-solid interface mediated by two-dimensional nucleation from supersaturated liquid alloy; (iv) growth of the substrate surface; and (v) the time dependence of the alloy supersaturation in the drop. Additionally, the transition from mononuclear to polynuclear growth modes at the liquid-solid interface [26–28] and the variation of NW radius during the growth will be incorporated into the model. The latter allows us to access the effect of NW tapering [22,29]. Possible shapes of the length-diameter dependence of NWs will be discussed and compared to earlier theoretical [14,19,23,26–28] and experimental [21,23,28,30,33,34] findings. We will discuss the theoretical dependence of NW length on the growth temperature. The final result will be the theoretical representation of NW morphology as a function of technologically controlled conditions of the NW fabrication procedure. This study completes our previously obtained results on the adsorption-induced [28] and diffusion-induced [23] VLS growth of NWs.

II. THE GROWTH MODEL

The model of NW growth during MBE is schematized in Fig. 1. This model takes into account (i) the direct impingement of deposit atoms on the drop surface from the material flux of rate V (adsorption); (ii) the desorption from the drop; (iii) the diffusion flux of adatoms from the substrate surface toward the drop along the NW sidewalls; (iv) the nucleation and lateral growth of two-dimensional islands at the liquid-solid interface [Fig. 1(b)]; and (v) the growth of nonactivated surface at rate V_s. The driving force for the VLS growth is the supersaturation of liquid alloy in the drop, $\zeta = C/C_{eq} - 1$. Here, C is the volume concentration of deposit atoms in the alloy (e.g., Si in Au-Si, Ga in Au-Ga) and C_{eq} is the temperature-dependent equilibrium concentration. We assume that all atoms arriving at the drop, irrespective of their pathway to it, are first dissolved in the drop and then either reevaporate or attach to the crystal lattice. The mechanism of this attachment is constituted by two-dimensional nucleation from the supersaturated alloy. Two-dimensional nuclei of the crystal phase arise, grow, and coalesce to build up a continuous layer on the NW top. Reiterative building of successive layers leads to the layer-by-layer vertical growth of the NW [16,26–28]. In contrast to previous theoretical studies [14,18,19,22,23,26–28] we allow the supersaturation ζ and, consequently, all other characteristics of the growth process to vary with time t. Also, the drop radius R is allowed to vary

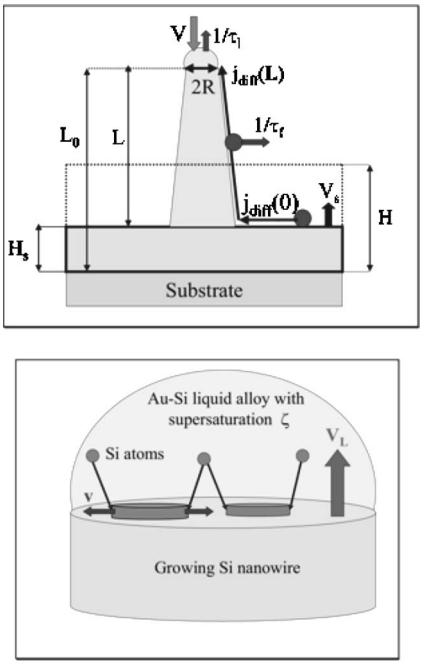

FIG. 1. Schematics of NW growth during MBE: (a) adsorption, desorption, adatom diffusion to the drop, and the growth of the substrate surface; the NW length $L=L_0-H_s$; (b) nucleation-mediated layer-by-layer growth on the liquid-solid interface, where v is the lateral growth rate of islands and $V_L=dL_0/dt$ is the outgoing flux of deposit atoms from the drop due to solidification of the liquid alloy (the example is Au-assisted growth of Si NWs).

during the growth, because it is directly related to the number of deposit particles in the drop. We assume, however, that the number of catalyst particles remains constant during the growth. This is an idealized case, because in Ref. [35] it has been demonstrated that gold might migrate on the sidewalls of Si NWs. If $N_0=\text{const}$ is the number of catalyst atoms (e.g., Au) and N is the number of deposit atoms (e.g., Si or Ga) in the drop, then $x=N/(N_0+N)$ is the concentration of deposit atoms in the alloy. Assuming, for simplicity, that the drop is a hemisphere with radius R and that the catalyst and the deposit atoms occupy the same volume Ω_l in the liquid phase, the drop volume equals $\Omega_{drop}=(2/3)\pi R^3=(N_0+N)\Omega_l$. The alloy concentration equals $C=N/\Omega_{drop}=x/\Omega_l$ and, therefore, supersaturation $\zeta=C/C_{eq}-1=x/x_{eq}-1$, where $x_{eq}=C_{eq}\Omega_l$ is the equilibrium concentration of the alloy. Using the equation $V(1-x)=(2/3)\pi R_0^3$, where $R_0=N_0\Omega_l=\text{const}$ is the radius of the pure catalyst drop at $N=0$, we arrive at the following relationship between R and ζ:

$$R=\frac{R_0}{[1-x_{eq}(\zeta+1)]^{1/3}}. \tag{1}$$

Generally, the number of semiconductor particles in the drop N changes in time due to the four processes shown in Fig. 1. The corresponding terms in the kinetic equation for $dN/dt=(2\pi R^2 dR/dt)/\Omega_l$ are described below.

(i) Adsorption on the drop surface. This term equals $\pi R^2 V/\Omega_s$, where $\Omega_s=\sigma h$ is the volume per atom in the crys-

tal, σ is the area per atom on the crystal surface, and h is the height of a monolayer (ML).

(ii) Desorption from the drop surface. This term equals $-2\pi R^2 r_l C_{eq}(\zeta+1)/\tau_l$, where r_l is the interatomic distance in the liquid and τ_l is the mean lifetime of deposit atoms in the drop.

(iii) Diffusion to the drop from the substrate surface along the sidewalls. This contribution is given by

$$j_{diff}(L) = -D_f n_{eq}^f 2\pi R \left.\frac{d\eta}{dz}\right|_{z=L}. \tag{2}$$

Here, D_f is the diffusion coefficient of the adatom on the sidewalls, n_{eq}^f is the adatom equilibrium concentration on the sidewalls, and η is the adatom supersaturation on the sidewalls. To estimate the diffusion flux of adatoms from the substrate surface to the NW base $j_{diff}(0)$, we assume that it is proportional to the perimeter of the base. In this case

$$j_{diff}(0) = \frac{R}{\langle R\rangle N_W} J_\Sigma \tag{3}$$

with $\langle R\rangle$ being the mean base diameter of the NW array, N_W the surface density of the NW array (both dictated by the size distribution of the initial drops), and J_Σ the overall diffusion flux from the substrate surface to the NW sidewalls per unit surface area. One the other hand, at typical MBE growth temperatures the desorption from the substrate surface is rather small. Therefore, the difference between the deposition rate V and the growth rate of the substrate surface V_s is caused mainly by the diffusion of adatoms to the NW sidewalls. In this case one can write

$$J_\Sigma = \frac{V - V_s}{\Omega_s}. \tag{4}$$

Comparing Eqs. (3) and (4), we find the expression for $j_{diff}(0)$,

$$j_{diff}(0) = \frac{V}{\Omega_s}\frac{\varepsilon R}{\langle R\rangle N_w}. \tag{5}$$

Here, $\varepsilon=(V-V_s)/V=(H-H_s)/H$ is the relative difference between the deposition rate and the growth rate of the substrate surface. This parameter is assumed below as being time independent. Implementing Eq. (5) as boundary condition for the kinetic equation for supersaturation η at $z=0$ and following the procedure described in detail in Ref. [23], the final result for the diffusion flux takes the form

$$j_{diff}(L) = 2\pi R\beta\left(\frac{1}{\cosh(\lambda)} - c(\zeta+1)\tanh(\lambda)\right). \tag{6}$$

Here, $\lambda \equiv L/L_f$ is the ratio of whisker length L to the adatom diffusion length on the side surface, $L_f=\sqrt{D_f\tau_f}$, D_f is the corresponding diffusion coefficient, and τ_f is the mean lifetime of the adatom on the NW sidewalls. The coefficients β and c are given by

$$\beta = \frac{V}{\Omega_s}\frac{\varepsilon}{2\pi\langle R\rangle N_W}, \quad c = \frac{2\pi\langle R\rangle N_W \theta_f L_f}{\varepsilon(V/h)\tau_f}, \tag{7}$$

with $\theta_f=\sigma n_{eq}^f$ being the equilibrium adatom coverage on the sidewalls and V/h the deposition rate in ML/s.

(iv) Atom sink at the liquid-surface interface. This term equals $-\pi R^2 V_L/\Omega_s$, where $V_L=dL_0/dt$ and L_0 is the NW length measured from the bare substrate (Fig. 1). In nucleation-mediated layer-by-layer growth, the vertical growth rate V_L is a certain function of nucleation rate I, lateral growth rate of islands v, and face radius R [26]. When R is very large, many nuclei arise in one layer, and then grow and coalesce to form a continuous film, while the boundary effects can be neglected. This situation takes place when the value of the parameter

$$\alpha = \pi I R^3/\nu \tag{8}$$

is large. Such growth is usually referred to as the polynuclear mode of nucleation-mediated growth. Vertical growth rate in the polynuclear mode is R independent. When, however, the face is sufficiently small, only one nucleus covers the whole face before the next nucleus is created, and the growth proceeds in the so-called mononuclear mode. In this mode, the value of the parameter α is small. The vertical growth rate is v independent. Transition from the mononuclear to the polynuclear mode of crystal growth can be described by the Kashchiev (K) formula [26,27]

$$V_L = h\frac{\pi I R^2}{1 + (\sqrt{3}\pi I/\nu)^{2/3} R^2}. \tag{9}$$

Another formula for $V_L(I,\nu,R)$ based on the generalized Kolmogorov-Johnson-Mehl-Avrami (GKJMA) model with boundaries has been proposed in Ref. [28]:

$$V_L = \frac{h\nu}{R y_*(\alpha)}. \tag{10}$$

The quantity $y_*(\alpha)$ here is determined as the solution to the transcendent equation

$$\alpha f(y) = 1 \tag{11}$$

with the function $f(y)$ given by

$$f(y) = \begin{cases} (1/3)y^3 - (3/32)y^4 - (1/80)y^5 + (1/192)y^6, & y \leqslant 2, \\ y - 0.9, & y > 2. \end{cases} \tag{12}$$

Equations (9)–(12) provide the asymptotic matching to the well known limit cases of pure mononuclear and pure polynuclear modes of nucleation-mediated growth [26]

$$V_L = \begin{cases} h\pi R^2 I, & \alpha \ll 1, \\ h(\pi\nu^2 I/3)^{1/3}, & \alpha \gg 1. \end{cases} \tag{13}$$

The Kashchiev and GKJMA expressions for V_L can be presented in the unified form

$$V_L = \pi R^2 I F(\alpha), \quad F(\alpha) = \begin{cases} 1/(1+3^{1/3}\alpha^{2/3}), & K, \\ 1/\alpha y_*(\alpha), & \text{GKJMA}. \end{cases} \tag{14}$$

Generally, the nucleation rate and the island growth rate depend on the supersaturation ζ. The simplest expressions of nucleation theory in the case of crystal growth from liquid alloys are given by [26,28,31]

$$I(\zeta) = \frac{1}{\sqrt{\pi}} \frac{1}{\sigma t_G} (\zeta + 1) \sqrt{\Delta\mu} \exp(-a/\Delta\mu), \tag{15}$$

$$\nu = \frac{\sqrt{\sigma}}{t_G} \zeta. \tag{16}$$

Here, $t_G = t_l / C_{eq} \Omega_l$ is the characteristic time of island lateral growth and t_l is the characteristic diffusion time in the liquid. The parameter a in Eq. (16) is determined by the specific interfacial energy of the liquid-solid boundary per unit length ε_{ls} and the surface temperature T according to

$$a = \pi\sigma \left(\frac{\varepsilon_{ls}}{k_B T} \right)^2. \tag{17}$$

Normally, the value of parameter a is quite large (more than 10) [31]. The difference in chemical potentials of the deposit atoms in the liquid and the solid phases, $\Delta\mu$ (expressed in $k_B T$ units), is a certain function of supersaturation ζ. For a diluted alloy

$$\Delta\mu = \ln(\zeta + 1). \tag{18}$$

However, this formula cannot be used at high concentration x, when the alloy is nonideal. The simplest way to expand Eq. (18) is to use the mean field approximation for a lattice gas with attractive interactions with potential $V(r)$ described by the interaction constant $\varphi = -\Sigma_r V(r)$ [32]. The size-dependent Gibbs-Thomson effect leads to a radius-dependent correction to $\Delta\mu$ of the form $-R_c/R$, where $R_c = 2(\Omega_s \gamma_{sv} - \Omega_l \gamma_{lv})/k_B T$ is the characteristic radius determined by the difference of surface energies of solid-vapor (γ_{sv}) and liquid-vapor (γ_{lv}) interfaces [28]. Hence, Eq. (18) is generalized to

$$\Delta\mu = \ln\left(\frac{x}{1-x} \right) - \varphi x - \frac{R_c}{R}. \tag{19}$$

Collecting all contributions together, we arrive at the following kinetic equation of NW growth:

$$\frac{2\pi R^2}{\Omega_l} \frac{dR}{dt} = \pi R^2 \frac{V}{\Omega_s} - 2\pi R^2 \frac{r_l C_{eq}}{\tau_l} (\zeta + 1) - \pi R^2 \frac{V_L}{\Omega_s} + j_{diff}(L). \tag{20}$$

The influence of substrate growth at rate $V_s = dH_s/dt$ is taken into account by the equation for the NW growth rate dL/dt following from the relationship $L = L_0 - H_s$ (Fig. 1) and the definition for the parameter ε:

$$\frac{dL}{dt} = V_L - (1 - \varepsilon) V. \tag{21}$$

In Eq. (20), the dependence $V_L = V_L(R, \zeta)$ is given by Eq. (14) with functions $\alpha(R, \zeta)$ defined in Eq. (8), $I(\zeta)$ in Eq. (15), and $\nu(\zeta)$ in Eq. (16). Diffusion flux to the drop $j_{diff}(L)$ is a function of R, ζ, and $\lambda = L/L_f$ given by Eq. (6) with coefficients (7). To make Eq. (20) closed, the relationship between the drop radius R and the alloy supersaturation ζ given by Eq. (1) should be used. Solving Eq. (20) numerically, we can find $R(t)$ and, therefore, all other characteristics of the NW growth process as functions of time t. Numerical integration of Eq. (21) gives the NW length as a function of NW radius and the MBE growth conditions.

The kinetic equation (20) can be presented in the following nondimensional form:

$$\frac{1}{V_*} \frac{dR}{dt} = (\Phi + 1) \left(1 + \frac{R_1}{R \cosh(\lambda)} \right) - (\zeta + 1) \left(1 + \frac{R_2}{R} \tanh(\lambda) \right) - \left(\frac{R}{R_3} \right)^2 G(\zeta) F(\alpha) \tag{22}$$

with the function $F(\alpha)$ defined in Eq. (14) and the functions $G(\zeta)$ and $\alpha(\zeta, R)$ given by

$$G(\zeta) = (\zeta + 1) \sqrt{\Delta\mu(\zeta)} \exp\left(-\frac{a}{\Delta\mu(\zeta)} \right), \tag{23}$$

$$\alpha(\zeta, R) = \sqrt{\pi} \left(\frac{R}{\sqrt{\sigma}} \right)^3 \frac{G(\zeta)}{\zeta}. \tag{24}$$

The resulting expression for the NW growth rate reads

$$\frac{dL}{dt} = V_0 \left[\left(1 + \frac{R_1}{R \cosh(\lambda)} \right) (\Phi + 1) - \left(1 + \frac{R_2}{R} \tanh(\lambda) \right) (\zeta + 1) - \frac{1}{V_*} \frac{dR}{dt} \right] - (1 - \varepsilon) V. \tag{25}$$

The growth process is therefore controlled by the following parameters: (1) Supersaturation of the gaseous phase

$$\Phi = \frac{V \tau_l}{2 r_l \Omega_s C_{eq}} - 1; \tag{26}$$

(2) radii R_1 and R_2 describing the diffusion-induced contributions to the NW growth rate

$$R_1 = \frac{\varepsilon}{\pi \langle R \rangle N_W}, \quad R_2 = \frac{n_{eq}^f}{r_l C_{eq}} \frac{\tau_l}{\tau_f} L_f; \tag{27}$$

(3) radius R_3 standing for the contribution of nucleation-mediated layer-by-layer growth of the crystal face,

$$R_3 = \sqrt{\sigma} \left(\frac{\Omega_s}{\Omega_l} \frac{2 r_l}{\sqrt{\pi h}} \right)^{1/2} \left(\frac{t_l}{\tau_l} \right)^{1/2}; \tag{28}$$

(4) the energetic parameter a defined in Eq. (17); (5) the parameter ε describing the growth of nonactivated substrate surface; (6) the parameter φ describing the interatomic interaction in the liquid alloy, when the system metastability $\Delta\mu$ is given by Eq. (19); (7) the Givargizov-Chernov size R_c describing the Gibbs-Thomson correction for the finite curvature of the NW and the drop surfaces in Eq. (19); (8) the kinetic parameters

$$V_0 = \frac{2r_l\Omega_s C_{eq}}{\tau_l} = \frac{V}{(\Phi+1)} \tag{29}$$

and $V_* = (\Omega_l/2\Omega_s)V_0 \approx V_0/2$; (9) the equilibrium alloy concentration x_{eq} and the number of catalyst atoms in the drop N_0; (10) the adatom diffusion length on the NW sidewalls L_f; (11) lattice geometry given by the lattice spacing $\sqrt{\sigma}$ and the height of a ML h; and (12) the deposition thickness $H=Vt$, or the deposition time t.

Among these parameters, for a particular material system at fixed temperature, the supersaturation Φ is controlled by the deposition rate, the parameters ε and the characteristic radius R_1 are controlled by the deposition rate and by the preparation procedure of the seed drops, and all other parameters are fixed. The temperature behavior of the system is more complex, since all the parameters described strongly and differently depend on the growth temperature.

The presented model of NW formation, to the best of our knowledge, in the most general form combines the ideas of the traditional VLS growth controlled by the direct impingement of deposit particles [14,17,28], of the Gibbs-Thomson correction for the finite curvature of the surface [14,28], of the diffusion-induced NW growth in systems with high surface diffusivity [18,19,23], and of the nucleation-mediated growth at the liquid-solid interface with allowance for the transition from mononuclear to polynuclear growth modes [26–28]. Since the model is essentially dynamical, it can describe various nonstationary effects during the NW growth, in particular, the transition between different growth regimes, the shape transformation and the tapering of NWs, and the time dependence of the alloy concentration in the drop. At a given size distribution of the initial eutectic drops, under certain assumptions on the temperature behavior of the system parameters (equilibrium concentrations, diffusion lengths, evaporation rates) and on the character of growth on the substrate surface, the model can predict the dependences of NW morphology on the technologically controlled growth conditions. The important information here is the dependence of NW length L on its radius R, growth temperature T, and deposition thickness H. Below we will discuss these dependences and compare our theoretical results to the available experimental data on the Si [21] and the GaAs [28–30,33,34] NWs.

III. RESULTS AND DISCUSSION

A. Limit regimes of NW formation

In order to qualitatively analyze different scenarios of NW growth, consider the typical values of model parameters during MBE of GaAs NWs [23]: $V/h \sim 1$ ML/s, $\tau_f \sim 1$ s, $\theta_f = \sigma n_{eq}^f \sim 10^{-3}$, $L_f \sim 10$ μm, $N_W \sim 10^9$ cm^{-2}, $\langle R\rangle \sim 100$ nm. In this case the value of the constant c in the right hand side of Eq. (6) equals $\sim 1/16\varepsilon$. The ratio between the second and the first terms in Eq. (6) $c(\zeta+1)\sinh(\lambda)$ at $\zeta+1\sim 1$ equals $\sim \sinh(\lambda)/16\varepsilon$. Taking for the estimate the values $\varepsilon=0.5$ and $L=5$ μm (relating to $\lambda=0.5$), we make sure that the second contribution to the adatom diffusion flux in Eq. (6) is approximately 15 times smaller than the first one. In this case one can neglect the term containing $\tanh(\lambda)$ in the right hand side of Eq. (25) for the NW growth rate. Obviously, this term is always small at $\lambda \ll 1$. If we also neglect the time dependence of the drop radius R, the steady-state equation (25) is simplified to

$$\frac{dL}{dt} = V_0(\Phi-\zeta) - (1-\varepsilon)V + V\frac{R_1}{R\cosh(\lambda)}. \tag{30}$$

The first term here describes the adsorption-desorption processes on the drop surface, the second term accounts for the substrate growth, and the third term stands for the incoming adatom diffusion flux from the sidewalls. The value of the first two terms in the right hand side of Eq. (30) is always smaller than the deposition rate $V=V_0$ $(\Phi+1)$. Equation (30) contains the known limit regimes of NW formation, briefly discussed below.

1. VLS growth controlled by the direct impingement of atoms on the drop surface

This limit regime follows Eq. (30) at $R_1/R\cosh(\lambda) \gg 1$, i.e., for very thick (large R) whiskers, very tall (large λ) wires, or at $\varepsilon \to 0$ (zero diffusion flux from the substrate surface, $R_1=0$), when the diffusion-induced contributions vanishes. In this regime the NW growth process is described by equations similar to those obtained in Ref. [28]:

$$\left(\frac{R}{R_3}\right)^2 G(\zeta)F(\alpha(\zeta,R)) = \Phi - \zeta, \tag{31}$$

$$\frac{dL}{dt} = V_0(\Phi-\zeta) - (1-\varepsilon)V. \tag{32}$$

Solving Eq. (31) for ζ, we obtain the $\zeta(R)$ dependence and then find the NW growth rate as a function of R from Eq. (32). As was shown previously in [14,26–28], the NW length in this regime generally increases with the radius, thicker whiskers thus growing faster than thinner ones. It should be noted here that the adsorption-induced VLS growth can be further divided into two submodes. The first submode takes place at a modest supersaturation of gaseous phase, when $\Phi \sim \zeta$. In this case the limiting stage of NW formation is the processes on the liquid-surface interface, i.e., the nucleation-mediated layer-by-layer growth [11,14]. The NW growth rate is quite low and rapidly decreases for smaller drops. Due to the Gibbs-Thomson effect, there exists a certain minimum radius of drop R_{min}, below which the NWs will not grow [11,14,28]. However, this critical radius decreases at higher supersaturation Φ. In MBE growth, one can anticipate that R_{min} is well below the technologically interesting range of drop sizes. In contrast, when the vapor supersaturation is very large $(\Phi \gg \zeta)$, the wire formation is controlled entirely by the adsorption-desorption processes on the drop surface. Looking at Eq. (32), at $\Phi \gg \zeta$ we do not require Eq. (31) at all, and, therefore, irrespective of ζ we arrive at the R-independent wire length

$$L = (\varepsilon - \gamma)H. \tag{33}$$

Here, $H=Vt$ is the effective thickness of deposited material. The coefficient $\gamma=V_0/V$ accounts for the desorption contribution and is given by

$$\gamma = \frac{2C_{eq}r_l\Omega_{s\xi}}{V\tau_l} \cong \frac{2x_{eq}}{(V/h)\tau_l}. \tag{34}$$

Obviously, Eq. (33) is the simplest form of material balance equation on the wire top, which should always hold for very thick wires.

2. Diffusion-induced growth of NWs

This limit regime is always realized when the diffusion flux of adatoms from the sidewalls is much larger than the deposition flux V. It follows from Eq. (30) at $R_1/R\cosh(\lambda) \gg 1$ and holds for sufficiently thin (small R) and sufficiently short NWs ($\lambda \ll 1$ and $\lambda \sim 1$). The adsorption-desorption contribution and the influence of substrate growth are negligible. The formula for the NW growth rate in this regime reads

$$\frac{dL}{dH} = \frac{R_1}{R\cosh(\lambda)}. \tag{35}$$

Here, $H=Vt$ is the effective thickness of deposited material. The solution to this equation with the initial condition $L(H=0)=0$ is given by

$$\sinh\left(\frac{L}{L_f}\right) = \frac{R_1 H}{RL_f}. \tag{36}$$

At small λ, i.e., for very short NWs or very large diffusion length of adatoms on the sidewalls, Eq. (36) is further simplified to

$$L = \frac{R_1}{R}H. \tag{37}$$

Therefore, the length of NWs growing primarily due to the adatom diffusion is inversely proportional to drop radius R and proportional to the effective thickness H. The $1/R$ dependence of whisker length was previously modeled, for example, in [18,19,23]. Such dependence was recently obtained experimentally in the case of Si NWs grown by MBE on the Si(111) surface activated by Au [21]. At large $R_1/R \gg 1$, the length of the thinnest NWs can be much higher than the effective thickness H. This effect was observed experimentally in the case of GaAs NWs grown by MBE on the GaAs(111)B-Au surface at 585 °C [23], where the length of 20–25 nm wide NWs was up to ten times higher than H.

In the case of very high supersaturation of the gaseous phase ($\Phi \gg \zeta$), irrespective of values of R_1 and λ, Eq. (30) is reduced to the formula obtained empirically in Ref. [23]:

$$\frac{dL}{dH} = \varepsilon - \gamma + \frac{R_1}{R\cosh(\lambda)}. \tag{38}$$

This equation is similar to Eq. (35) but contains an additional R-independent constant. Equation (38) provides a reasonable fit with the experimental $L(R)$ curves of GaAs NWs grown by MBE on the GaAs(111)B-Au surface [23]. At $\lambda \ll 1$, the integration of Eq. (38) gives

$$L = \left(\varepsilon - \gamma + \frac{R_1}{R}\right)H. \tag{39}$$

This equation fits well with the experimental $L(R)$ curves of GaAs NWs grown by magnetron sputtering deposition (MSD) on the GaAs(111)B-Au surface [34].

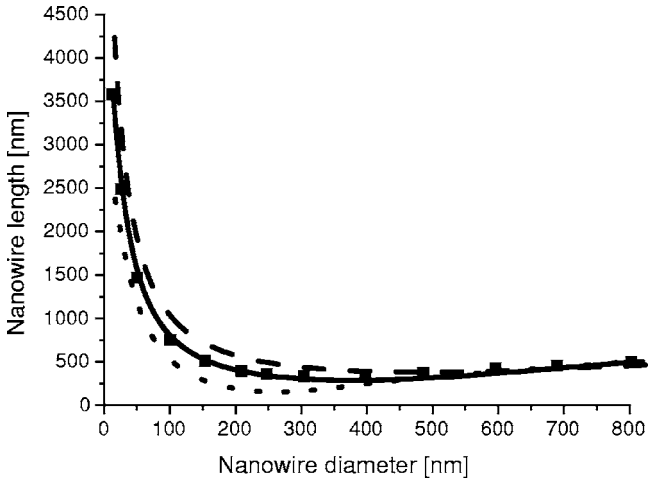

FIG. 2. Length-diameter dependences of NWs at $\Phi=15.7$ (lower curve), 26.8 (middle curve), and 37.9 (upper curve). The curves are calculated with the use of the Kashchiev model of nucleation-mediated growth of an arbitrary sized face. Black squares are the results obtained at $\Phi=26.8$ and the same model parameters with the use of the GKJMA model.

B. Shape of the length-diameter curves

Typical length-diameter dependences obtained from the numerical solution of dynamic equations (1) and (22)–(25) are presented in Fig. 2. The values of D in Fig. 2 relate to the diameters of NW tops immediately after the growth interruption at the effective thickness H, because generally $D(t)=2R(t)$ varies during the growth. During the simulations, the Gibbs-Thomson effect was not taken into account ($R_c=0$), since it is usually not important during MBE growth. In the case of CVD of very thin NWs, this term is significant and should be taken into account in Eq. (19). The calculations were performed for the fixed model parameters $R_1=R_2=90$ nm, $R_3=0.013$ nm, $a=11.5$, $\varphi=4$, $x_{eq}=0.1$, $L_f=5$ μm, $\varepsilon=0.8$, $\sigma=0.55$ nm^2, $h=0.33$ nm, at three different values of supersaturation of the gaseous phase $\Phi=15.7$, 26.8, and 37.9. These values of Φ at the given model parameters and at a constant growth temperature relate to the deposition rates $V/h=0.3$, 0.5, and 0.7 ML/s and to the surface growth rates $V_s=0.06$, 0.1, and 0.14 ML/s, respectively. The effective thickness of deposited material H was fixed to 700 nm. From Fig. 2 it is seen that the length-radius dependence for sufficiently thin NWs is always decreasing and can often be described by the k_1+k_2/R approximation given by Eq. (39). At small drop radius, the NW growth is controlled mainly by the adatom diffusion, and their maximum length is 3.5–6.5

times larger than H. These results agree well with previous experimental findings in the case of MBE growth of Si [21], MBE growth of GaAs [23], and MSD growth of GaAs [34] NWs. Quantitative comparison of theoretical and experimental $L(R)$ dependences for the diffusion-induced growth of GaAs NWs can be found in Refs. [23,34].

When the lateral size of drops increases, theoretical length-diameter curves converts from decreasing to slightly increasing, as demonstrated by Fig. 2. The $L(D)$ dependences obtained have therefore a minimum at a certain diameter D_*. This diameter increases with supersaturation Φ (at fixed ratio between the deposition rate and the substrate growth rate). For the model parameters described, the value of D_* varies approximately from 200 to 400 nm. As follows from Fig. 2, the minimum of $L(D)$ curves becomes more pronounced at smaller values of Φ and almost vanishes at sufficiently high Φ. This conversion effect can be explained by the transition from diffusion-induced to the adsorption-induced VLS growth discussed above. At sufficiently large R, all contributions from the adatom diffusion must vanish approximately as $1/R$, and the NW growth is controlled primarily by the two-dimensional nucleation on the liquid-solid interface. The increase in the length-diameter dependence for larger drops is associated with the transition from the mononuclear to the polynuclear growth mode [26–28]. Since in the mononuclear mode the nucleation-mediated growth rate is proportional to R^2 and in the polynuclear mode goes to a constant, the NWs are bound to grow at an increasing R-dependent rate. Theoretical dependences calculated at the same model parameters with the use of the Kashchiev [26] and GKJMA [28] models do not demonstrate any considerable difference between them (Fig. 2).

The transition from decreasing to increasing length-diameter dependence at a certain critical diameter is indirectly supported by earlier experimental results on MBE-grown GaAs NWs. As already discussed, the experimental decreasing $L(D)$ curve for GaAs/GaAs(111)B-Au NWs within the range of diameters from 20 to 150 nm is well described by the diffusion-induced model given by Eq. (38) [23]. The MBE growth experiment of Ref. [23] was performed at 1.0 nm thickness of the initial Au layer d_{Au}. heated up to the temperature of 630 °C. The growth temperature T amounted to 585 °C, the deposition rate of GaAs V/h was 1.0 ML/s, and the flux ratio of As_4 to Ga was 1.0. When, however, the MBE growth was performed at similar conditions but with larger thickness of the Au layer $d_{\mathrm{Au}}=2.5$ nm (the maximum NW diameter thus reached 400 nm) and at lower deposition rate $V/h=0.5$ ML/s, the observed $L(R)$ dependence was increasing [30]. The direct measurement of critical size D_* and the quantitative treatment of the transition between the two growth modes requires a more precise experimental study. The general conclusion here is that, depending on the drop size and on the MBE growth conditions, one can observe either the diffusion-induced or the traditional adsorption-induced VLS growth of whiskers, characterized by qualitatively different length-radius curves. At a wider range of drop sizes, the transformation between the two growth modes, one with decreasing and the other with increasing $L(R)$ dependence, can be observed.

C. Temperature behavior of NW length

To study qualitatively the dependence of NW length on the technologically controlled growth conditions, consider the simplest equation describing the growth of the substrate surface:

$$\frac{dn_s}{dt}=\frac{V}{\Omega_s}-\frac{n_s}{\tau_s}-N_w 2\pi\langle R\rangle\frac{l_s}{t_s}n_s-\frac{1}{\sigma}\frac{dg}{dt}. \tag{40}$$

The surface concentration of adatoms n_s changes in time due to (i) the arrival of atoms from a molecular beam with rate V, (ii) the desorption with mean stay time τ_s, (iii) the outgoing flux to NWs ($l_s\sqrt{\sigma}$ is the length of adatom diffusion jumps and t_s is the characteristic time between the jumps), and (iv) the nucleation and growth of the two-dimensional layer (g is the time-dependent coverage of the surface). In Eq. (40) we assume that the flux to the NW base is proportional to the overall perimeter of NWs $N_W 2\pi\langle R\rangle$ and to the adatom concentration n_s. As is known [31,36], if the lateral growth rate of islands di/dt (expressed in terms of number of atoms in the island i) is proportional to i^m, where $0<m<1$, the adatom concentration at the final stage of continuous layer formation goes to its equilibrium value $n_s\rightarrow n_{eq}^s$. In this case we should put $dn_s/dt=0$ in Eq. (40) and therefore $g(t)\rightarrow(V/h-\theta_s/\tau_{eff})t$. Here, $\theta_s=\sigma n_{eq}^s$ is the equilibrium adatom coverage of the substrate surface, τ_{eff} is the renormalized desorption time defined as $1/\tau_{eff}=(2\pi\langle R\rangle N_W l_s/t_s)(1+\delta)$, and $\delta\equiv t_s/2\pi\langle R\rangle N_W l_s\tau_s$ is the ratio between the probability of adatom desorption and the probability of adatom jump to the sidewalls. Normally, the value of δ is very small. The ML reaches continuity at $g(t_{ML})=1$, the time of ML formation t_{ML} is found from $(V/h-\theta_s/\tau_{eff})t_{ML}=1$, while the surface growth rate obviously equals $V_s=h/t_{ML}$. For the parameter ε this yields $\varepsilon=\theta_s h/V\tau_{eff}$. Using Eq. (43) in Eq. (27) for R_1, we arrive at

$$R_1=\frac{2\theta_s l_s h}{Vt_s}(1+\delta)\propto\exp\left(-\frac{\psi_s+E_D^s}{k_BT}\right). \tag{41}$$

Here, we depict explicitly the temperature dependence of R_1 following from the temperature dependences of θ_s and t_s: $\theta_s\sim\exp(-\psi_s/k_BT)$ and $t_s\sim\exp(E_D^s/k_BT)$, ψ_s being the specific condensation heat of adatoms and E_D^s the activation energy for their diffusion jump [31]. Equation (41) shows that the characteristic radius R_1, describing the diffusion from the substrate surface to the NW sidewalls, increases with the growth temperature T as the Arrhenius exponent.

In the diffusion-induced mode of NW formation, typical for the MBE growth of NWs on the surface with sufficiently small seed drops, the NW length is given by Eq. (36) or (38). The temperature dependence of NW length at fixed R, H, and V is governed by the temperature dependence of R_1 given by Eq. (41) and the temperature dependence of the adatom diffusion length $L_F\propto\exp[(E_A^f-E_D^f)/2k_BT]$, where E_A^f and E_D^f are the activation energies for the adatom desorption and diffusion on the sidewalls. When the growth is described by Eq. (38), the temperature dependence of the desorption term $\gamma\propto\exp[-(\psi_l+E_A^l)/k_BT]$ should also be taken into account, where ψ_l is the specific condensation heat in the liquid and

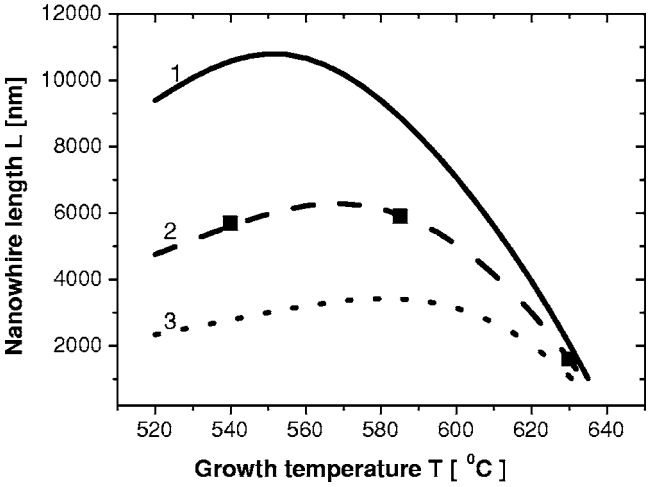

FIG. 3. Temperature dependence of NW length obtained from Eq. (38) at three different NW radii: $R=10$ (1), 20 (2), and 40 nm (3), for the model parameters described in the text. Black squares are corresponding experimental points in the case of MBE-grown GaAs/GaAs(111)B-Au NWs from Ref. [33].

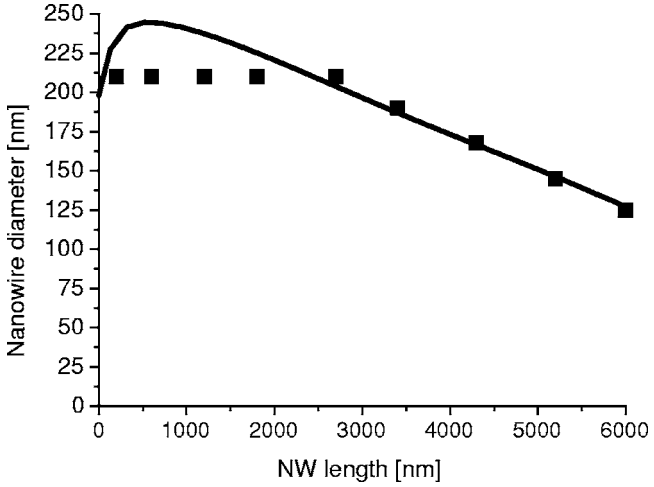

FIG. 4. Dependence of NW diameter on its length. Solid curve, theory; square points, experimental results for GaAs NWs [29].

E_A^l is the activation energy for desorption from the drop. Consider, for simplicity, Eq. (36) for the NW length. At very low surface temperatures adatoms will not evaporate from the sidewall and will all reach the NW top. This relates to the case of $L/L_f \ll 1$described by Eq. (37). The $L(T)$ dependence at low temperatures is therefore dictated by the temperature dependence of R_1:

$$L \propto R_* \propto \exp\left(-\frac{\psi_s + E_D^s}{k_B T}\right), \quad \text{low } T. \tag{42}$$

The increase of temperature induces faster diffusion on the surface and increases the equilibrium concentration of adatoms. These two effects increase the diffusion flux to the NW base, and consequently to the NW top, at a low desorption rate from the sidewalls. Therefore, at low temperatures the $L(T)$ dependence should be increasing.

In contrast, at high temperatures the adatom flux to the NW top is mainly limited by the reevaporation from its sidewalls. This is the case of $L/L_f \gg 1$, for which Eq. (36) is reduced to

$$L \to L_f \ln\left(\frac{R_1 H}{R L_f}\right) \propto \exp\left(\frac{E_A^f - E_D^f}{2k_B T}\right), \quad \text{high } T. \tag{43}$$

At high temperatures the $L(T)$ dependence is dictated mainly by the temperature dependence of L_F, only logarithmically depends on the ratio R_1/L_F, and, therefore, converts to a decreasing curve. This simple analysis shows that the $L(T)$ dependence should reach a maximum at a certain temperature T_{opt}, which is the optimal temperature for the fabrication of the longest NWs at otherwise the same growth conditions.

Typical temperature dependences of the NW length in the diffusion-induced mode of NW formation are presented in Fig. 3. The curves were obtained by the integration of Eq. (38) at three different $R=$const, constant deposition thickness $H=800$ nm, $L_f(585\ ^\circ\text{C})=5\ \mu$m, and $R_1(585\ ^\circ\text{C})=450$ nm. The temperature dependences of R_1, L_f, and γ were taken in the Arrhenius forms described above at the model values of $\psi_s+E_D^s=0.55$ eV, $E_A^f-E_D^f=2.7$ eV, $\psi_l+E_D^l=2.9$ eV. The curve at $R=40$ nm provides a good fit with the experimental results obtained for the GaAs NWs grown by MBE with constant $H=800$ nm [34]. It is seen that the optimal temperature corresponding to the longest NWs with radii from 20 to 80 nm in our example occurs within the range from 550 to 600 °C.

D. Tapering of nanowhiskers

In a recent experimental study of the VLS mechanism of GaAs/GaAs(111)B-Au NW growth by MBE [29], it has been demonstrated that the NWs grown at 590 °C taper beginning from a length of about 3 μm. The NWs have the same cylindrical shape within the first 3 μm of their length, but then taped at an approximately constant rate of about 25 nm per 1 μm length, as demonstrated by the experimental curve in Fig. 4. The explanation of this effect, qualitatively discussed in Ref. [29], can be given within the frame of the dynamical model described by Eqs. (1) and (22)–(24).

As already discussed, there exist two different Ga fluxes to the drop. One flux directly impinges on the catalyst and the other is promoted by the adatom diffusion from the substrate surface to the top of the NWs. During the deposition at constant growth conditions, the impingement flux on the drop remains the same and the diffusion flux decreases due to adatom evaporation from the sidewalls. The reduction of this flux becomes very pronounced when the length L reaches the mean diffusion length of Ga atoms. Therefore, at $L/L_f \ll 1$ the system consisting of the NW, the drop, and the Ga-supplying fluxes is in a steady state with a higher Ga concentration in the alloy, while at $L/L_f \sim 1$ the system evolves toward a new state. The Ga concentration in the alloy, and consequently the radius of the drop, must decrease, which induces a diminution of the NW lateral size.

The theoretical $D(L)$ curve obtained from Eqs. (1) and (22)–(24) at $R_1=450$ nm, $R_2=45$ nm, $R_3=0.08$ nm, $a=11.5$, $\varphi=4$, $x_{eq}=0.1$, $L_f=3\ \mu$m, $\sigma=0.55$ nm^2,

$h=0.33$ nm, $V/h=0.61$ ML/s, $\Phi=7.5$, and $H_{eff}=1920$ nm provides a qualitative agreement with the experimental data. However, unlike the experimental curve, the theoretical $D(L)$ curve increases at the initial stage of growth, because the Ga concentration in the alloy should first increase to reach supersaturation sufficient to induce the VLS growth. This effect was not observed experimentally in [29], but looks theoretically feasible. Such increase of Ga concentration would lead to a certain widening of the NW bases. Also, according to the x-ray energy dispersive analysis of Ref. [29], when the NWs are grown without exposure to the arsenic flux after closing the Ga shutter, the concentration of Ga in the solid Au-Ga solution (measured after cooling) changes typically from 0.5 for short to 0.3 for long NWs. According to Eq. (1), such decrease of x cannot fully explain more than a two times decrease of the NW top diameter, observed in Ref. [29]. To fit the experimentally measured rate of tapering, the theoretical curve in Fig. 4 was therefore modeled to the wider range of $x=0.9$ for the maximum and $x=0.2$ for the minimum NW diameter. This leads to earlier tapering of the theoretical $D(L)$ curve in Fig. 4, because the dependence of $R(x)$ given by Eq. (1) becomes steeper as x approaches unity. According to Eqs. (14)–(16), the decrease of Ga concentration in the alloy lowers the NW growth rate and at $x=x_{eq}$ the VLS growth must be completely stopped. A gradual decrease of Ga concentration might lead to the solidification of the alloy and, consequently, to the transition from the VLS to the vapor-solid-solid mechanism described in Ref. [25]. The large decrease of NW lateral size, observed in Ref. [29], is probably not only induced by the Ga concentration effect described above, but also supported by changing the directions of interfacial forces for conically shaped NWs, modeled in Ref. [22]. The effect of cooling might also be significant for the tips of very long NWs, while the model in its present form assumes that the temperature along the NW length is the same as the surface temperature T. Finally, the drop might lose some of the Au [35], causing further decrease of its size.

According to our analysis, the tapering of GaAs NWs grown by MBE on the GaAs(111)B surface at $T=590$ °C can be explained by the reduction in the Ga-supplying flux to the drop due to the evaporation of Ga atoms from the sidewalls. Tapering due to the nucleation on the GaAs(110) sidewalls seems unlikely for the following reasons. Applying the nucleation theory [31,36], the activation barrier for the nucleation of two-dimensional islands (expressed in k_BT units) is given by $\Delta G=b/\ln(\eta+1)$, where η is the adatom supersaturation on the sidewalls. The parameter b is given by a formula similar to Eq. (17): $b=\pi\sigma(\varepsilon_{vs}/k_BT)^2$ with ε_{vs} being the specific energy of the vacuum-crystal interface per unit length of island boundary. Estimating ε_{vs} as $\varepsilon_{vs}\sim\gamma_{vs}h$, where γ_{vs} is the corresponding surface energy, and using the data of Ref. [37] for γ_{vs}, σ, and h, at $T=590$ °C, we get $b^{(111)}\sim b^{(110)}\sim 200$. Taking for estimates the typical value of maximum adatom supersaturation $\eta\sim 100$ [36], we obtain the value of $\Delta G\sim 42$ for both surfaces. The nucleation on the main (111) surface always proceeds in polynuclear mode, while the nucleation on the sidewalls of sufficiently thin NWs is mononuclear, because one nucleus immediately forms a ring around the NW. In the polynuclear mode the normal growth rate is proportional to $I^{1/3}$, and in mononuclear mode to I, where $I\sim\exp(-\Delta G)$ is the nucleation rate of islands [26,28]. Therefore, the ratio of normal growth rates on the (110) and (111) surfaces is of the order of $\exp(-2\Delta G/3)\sim 10^{-6}$. Note that in reality the adatom supersaturation on the sidewalls must be lower than on the (111) surface, because their difference drives the diffusion flux to the sidewalls. Hence, the actual difference in normal growth rates on the (110) and (111) surfaces is even larger and the vapor-solid growth in the direction perpendicular to the sidewalls can be neglected in our case. When, however, the widening of NWs becomes pronounced, the additional mechanism of the adatom sink on the sidewalls due to nucleation should be taken into consideration.

IV. CONCLUSIONS

The model developed in this work can describe different regimes of VLS growth of NWs during MBE and, after a certain modification, can also be applied to the case of CVD. The model describes several effects during NW formation, in particular the transition from increasing to decreasing length-radius dependence at a certain critical diameter, the time dependence of the alloy supersaturation, and the tapering of NWs. We have also analyzed the theoretical dependence of NW morphology on the technologically controlled growth conditions and derived a semiquantitative dependence of NW length on the growth temperature. Some of the model predictions, such as the existence of an optimal temperature to fabricate the longest NWs with the highest aspect ratio, the diffusionlike length-diameter dependence of sufficiently thin NWs, and the NW tapering at a length comparable to the diffusion length of adatoms on the sidewalls, are confirmed by the available experimental data obtained for different material systems [21,23,29,34]. Other effects, such as the conversion of length-diameter curves, at the moment remain mainly theoretical predictions and require a separate experimental study. Some additional improvements of the model are required to accomplish the complete kinetic description of NW growth. Among these, we would like to mention the detailed treatment of phase transitions in the alloy [25], the influence of the flux ratio in the case of III-V NWs, the study of the temperature distribution along the NW length, the investigation of catalyst diffusion from the drop, and faceting of the sidewalls [35]. The simulations of particular material systems requires the knowledge of many physical constants such as equilibrium concentrations, characteristic diffusion and desorption times, and interfacial energies. At the moment they are combined in several fitting parameters, whose physical sense is quite clear but the numerical values can only be roughly estimated. Nevertheless, the comparison of theoretical and experimental data allows us to obtain useful information concerning the physical values of rather complex material systems. In particular, the measured $D(L)$ dependence of tapered NWs enables us to estimate the diffusion length of adatoms [29], and the measured $L(D)$ and $L(H)$ curves pro-

vide numeric estimates for the adatom diffusion flux, the growth rate of the substrate surface, and the desorption rate from the drop surface [34]. In the overall view, the developed theoretical approach might help in better understanding of the controlled production of NWs with the desired morphological properties for different applications.

ACKNOWLEDGMENTS

The authors are grateful for the financial support received from the SANDiE program, RFBR Grants No. 05-02-16495, No. 05-02-16658 and No. 05-02-08090-OFI, a scientific grant of the St.-Petersburg Scientific Center, and different scientific programs of RAS.

[1] M. S. Gudiksen, L. J. Lauhon, J. Wang, D. C. Smith, and C. M. Lieber, Nature (London) **415**, 617 (2002).
[2] M. T. Björk, B. J. Ohlsson, T. Sass, A. I. Persson, C. Thelander, M. H. Magnusson, K. Deppert, L. R. Wallenberg, and L. Samuelson, Appl. Phys. Lett. **80**, 1058 (2002).
[3] Y. Cui and C. M. Lieber, Science **91**, 851 (2000).
[4] F. Patolsky, G. Zheng, O. Hayden, M. Lakadamyali, X. Zhuang, and C. M. Lieber, Proc. Natl. Acad. Sci. U.S.A. **101**, 14017 (2004).
[5] Y. Cui, L. J. Lauhon, M. S. Gudiksen, J. Wang, and C. M. Lieber, Appl. Phys. Lett. **78**, 2214 (2001).
[6] T. I. Kamins, X. Li, and R. S. Williams, Appl. Phys. Lett. **82**, 263 (2003).
[7] J. Westwater, D. P. Gosain, S. Tomiya, and S. Usui, J. Vac. Sci. Technol. B **15**, 554 (1997).
[8] C. Thelander, T. Martensson, M. T. Björk, B. J. Ohlsson, M. W. Larsson, L. R. Wallenberg, and L. Samuelson, Appl. Phys. Lett. **83**, 2052 (2003).
[9] Y. Xia, P. Yang, Y. Sun, Y. Wu, B. Mayers, B. Gates, Y. Yin, F. Kim, and H. Yan, Adv. Mater. (Weinheim, Ger.) **15**, 353 (2003).
[10] R. S. Wagner and W. C. Ellis, Appl. Phys. Lett. **4**, 89 (1964).
[11] E. I. Givargizov, J. Cryst. Growth **31**, 20 (1975).
[12] P. M. Petroff, A. C. Gossard, and W. Wiegmann, Appl. Phys. Lett. **45**, 620 (1984).
[13] R. Bhat, E. Kapon, S. Simhony, E. Colas, D. M. Hwang, N. G. Stoffel, and M. A. Koza, J. Cryst. Growth **107**, 716 (1991).
[14] E. I. Givargizov and A. A. Chernov, Kristallografiya **18**, 147 (1973).
[15] K. Hiruma, M. Yazawa, T. Katsuyama, K. Ogawa, K. Haraguchi, and M. Koguchi, J. Appl. Phys. **77**, 447 (1995).
[16] X. Duan and C. M. Lieber, Adv. Mater. (Weinheim, Ger.) **12**, 298 (2000).
[17] D. N. Mcllroy, A. Alkhateeb, D. Zhang, D. E. Aston, A. C. Marcy, and M. G. Norton, J. Phys.: Condens. Matter **16**, R415 (2004).
[18] J. M. Blakely and K. A. Jackson, J. Chem. Phys. **37**, 428 (1962).
[19] V. Ruth and J. R. Hirth, J. Chem. Phys. **41**, 31 (1964).
[20] S. Bhunia, T. Kawamura, S. Fujikawa, and Y. Watanabe, Physica E (Amsterdam) **24**, 238 (2004).
[21] L. Schubert, P. Werner, N. D. Zakharov, G. Gerth, F. M. Kolb, L. Long, U. Gösele, and T. Y. Tan, Appl. Phys. Lett. **84**, 4968 (2004).
[22] V. G. Dubrovskii, I. P. Soshnikov, G. E. Cirlin, A. A. Tonkikh, Yu. B. Samsonenko, N. V. Sibirev, and V. M. Ustinov, Phys. Status Solidi B **241**, R30 (2004).
[23] V. G. Dubrovskii, G. E. Cirlin, I. P. Soshnikov, A. A. Tonkikh, N. V. Sibirev, Yu. B. Samsonenko, and V. M. Ustinov, Phys. Rev. B **71**, 205325 (2005).
[24] A. Y. Cho and J. R. Arthur, Prog. Solid State Chem. **10**, 157 (1975).
[25] A. I. Persson, M. W. Larsson, S. Stengstrom, B. J. Ohlsson, L. Samuelson, and L. R. Wallenberg, Nat. Mater. **3**, 677 (2004).
[26] D. Kashchiev, *Nucleation: Basic Theory with Applications* (Butterworth Heinemann, Oxford, 2000).
[27] W. Obretenov, D. Kashchiev, and V. Bostanov, J. Cryst. Growth **96**, 846 (1989).
[28] V. G. Dubrovskii and N. V. Sibirev, Phys. Rev. E **70**, 031604 (2004).
[29] J. C. Harmand, G. Patriarche, N. Péré-Laperne, M. -N. Mérat-Combes, L. Travers, and F. Glas, Appl. Phys. Lett. **87**, 203101 (2005).
[30] A. A. Tonkikh, G. E. Cirlin, Yu. B. Samsonenko, I. P. Soshnikov, and V. M. Ustinov, Semiconductors **38**, 1217 (2004).
[31] K. Reichelt, Vacuum **38**, 1083 (1988).
[32] V. G. Dubrovskii, D. A. Bauman, V. V. Kozachek, V. V. Mareev, and G. E. Cirlin, Physica A **260**, 349 (1998).
[33] V. G. Dubrovskii, G. E. Cirlin, I. P. Soshnikov, N. V. Sibirev, Yu. B. Samsonenko, and V. M. Ustinov, Int. J. Nanosci. (to be published).
[34] V. G. Dubrovskii, G. E. Cirlin, I. P. Soshnikov, N. V. Sibirev, Yu. B. Samsonenko, and V. M. Ustinov, J. Cryst. Growth (to be published).
[35] F. M. Ross, J. Tersoff, and M. C. Reuter, Phys. Rev. Lett. **95**, 146104 (2005).
[36] V. G. Dubrovskii, Phys. Status Solidi B **171**, 345 (1992).
[37] *Adsorbed Layers on Surfaces. Part 1: Adsorption on Surfaces and Surface Diffusion of Adsorbates*, edited by W. Martienssen, Landolt-Börnstein, New series, vol. 42, pt. A1. (Springer, Berlin, 2001).